

Climate-model induced differences in the 21st century global and regional glacier contributions to sea-level rise

Rianne H. Giesen · Johannes Oerlemans

Received: 31 July 2012 / Accepted: 15 March 2013
© Springer-Verlag Berlin Heidelberg 2013

Abstract The large uncertainty in future global glacier volume projections partly results from a substantial range in future climate conditions projected by global climate models. This study addresses the effect of global and regional differences in climate input data on the projected twenty-first century glacier contribution to sea-level rise. Glacier volume changes are calculated with a surface mass balance model combined with volume-area scaling, applied to 89 glaciers in different climatic regions. The mass balance model is based on a simplified energy balance approach, with separated contributions by net solar radiation and the combined other fluxes. Future mass balance is calculated from anomalies in air temperature, precipitation and atmospheric transmissivity, taken from eight global climate models forced with the A1B emission scenario. Regional and global sea-level contributions are obtained by scaling the volume changes at the modelled glaciers to all glaciers larger than 0.1 km^2 outside the Greenland and Antarctic ice sheets. This results in a global value of $0.102 \pm 0.028 \text{ m}$ (multi-model mean and standard deviation) relative sea-level equivalent for the period 2012–2099, corresponding to $18 \pm 5 \%$ of the estimated total volume of glaciers. Glaciers in the Antarctic, Alaska, Central Asia and Greenland together account for $65 \pm 4 \%$ of the total multi-model mean projected sea-level rise. The projected sea-level contribution is $35 \pm 17 \%$ larger when only anomalies in air temperature are taken into account, demonstrating an important compensating effect by increased precipitation and possibly reduced atmospheric transmissivity. The variability in projected precipitation

and atmospheric transmissivity changes is especially large in the Arctic regions, making the sea-level contribution for these regions particularly sensitive to the climate model used. Including additional uncertainties in the modelling procedure and the input data, the total uncertainty estimate for the future projections becomes $\pm 0.063 \text{ m}$.

Keywords Glacier volume projections · Sea-level rise · Global climate models · Climate change

1 Introduction

Glacier volume changes have many implications on local and regional scales, for instance by affecting hydropower production, tourism and freshwater supply. Estimates of future glacier extent and discharge for individual glaciers and hydrological basins are therefore valuable (e.g., Stahl et al. 2008; Immerzeel et al. 2012). Since glaciers are expected to remain a major contributor of fresh water to the oceans in the twenty-first century (IPCC 2007), global glacier volume projections need to be taken into account in estimates of regional and global sea-level rise and ocean circulation changes (e.g., Landerer et al. 2007; Pardaens et al. 2010).

One of the major sources of uncertainty in glacier volume projections is the large spread in future climate conditions given by a suite of atmosphere-ocean general circulation models (AOGCMs, Oerlemans et al. 2005; Radić and Hock 2011; Slangen and van de Wal 2011). Glaciers are located in mountainous regions, which are not well resolved in the coarse-resolution AOGCMs. Although higher-resolution regional climate models (RCMs) are being applied to an increasing number of regions (e.g., Ettema et al. 2009; Urrutia and Vuille 2009; Heikkilä et al.

R. H. Giesen (✉) · J. Oerlemans
Institute for Marine and Atmospheric Research Utrecht, Utrecht University, P.O. Box 80 005, 3508 TA Utrecht, The Netherlands
e-mail: R.H.Giesen@uu.nl

2011), these do not yet cover all glacierized regions. Moreover, for consistency in the results, it is often preferred to use climate input from the same model for all regions.

Global glacier volume projections are based on simple models that only require air temperature and precipitation as input data (Raper and Braithwaite 2006; Radić and Hock 2011; Slangen et al. 2012) for two reasons. For most glaciers, the data needed to calibrate a more sophisticated energy balance model are not available. Moreover, as a consequence of the large spread in the future climate data produced by AOGCMs, model improvement does not considerably reduce the uncertainty in the projections. In the simple models, the energy exchange between the atmosphere and the glacier surface is highly parameterized. While these models may perform well for present-day conditions, they may not be suitable for future simulations, where the relative contribution to melt by the various surface energy fluxes may be different.

In this study, we use a model that separately computes the contributions by net solar radiation and the combined other fluxes to the surface energy balance, thereby providing an improved physical basis with respect to previously applied models in global glacier volume projections. The mass balance model is applied to 89 glaciers in different climatic regions of the world. Subsequently, the results are transferred to all glaciers and ice caps that are not part of the Greenland and Antarctic ice sheets (referred to as ‘glaciers’ in this paper) to provide global and regional contributions of glaciers to sea-level in the twenty-first century. Future glacier volume projections simulated with input data from eight climate models are presented and the spread in the results is related to the differences in modelled future climate. Furthermore, the separate calculation of net solar radiation in our model enables an analysis of the effect of future changes in surface albedo and atmospheric transmissivity on the glacier volume change.

2 Methods

The applied method consists of three parts, which are outlined in this section:

- the application of a mass balance model to 89 glaciers for which mass balance measurements are available to calibrate the model;
- the incorporation of changes in glacier geometry by means of volume-area scaling and a parameterization for the loss of area per elevation interval;
- the upscaling of the results for the 89 glaciers to all glaciers larger than 0.1 km² in the Randolph Glacier Inventory (RGI, Arendt and 77 others 2012).

2.1 Mass balance model

2.1.1 Model description

The mass balance model is described in detail by Giesen and Oerlemans (2012), here we only give a brief description of the main model characteristics. The annual surface mass balance (B) is given by

$$B = \int_{\text{year}} \left\{ P_{\text{snow}} + (1 - r) \min \left(0; -\frac{Q}{\rho_w L_f} \right) \right\} dt. \quad (1)$$

Accumulation at every altitude is determined from solid precipitation P_{snow} ; precipitation is assumed to fall as snow when the air temperature is below 1.5 °C. Melt is assumed to occur whenever the surface energy balance (Q) is positive and part of the meltwater r is allowed to refreeze within the snowpack. The constant L_f is the latent heat of fusion, ρ_w is the water density.

Surface melt is calculated from a simplified surface energy balance formulation where the melt energy (Q) is separated into contributions by net solar radiation (S_{net}) and all other fluxes (ψ), written as a function of air temperature (T_a):

$$Q = S_{\text{net}} + \psi \quad (2)$$

$$= (1 - \alpha) \tau S_{\text{in,TOA}} + \begin{cases} \psi_{\text{min}} + bT_a & \text{for } T_a \geq T_{\text{tip}}; \\ \psi_{\text{min}} & \text{for } T_a < T_{\text{tip}}. \end{cases} \quad (3)$$

Net solar radiation is computed by multiplying the incoming solar radiation at the top of the atmosphere ($S_{\text{in,TOA}}$) by the atmospheric transmissivity (τ) and subtracting the part of the incoming solar radiation reflected by the surface with albedo α . For τ we use monthly values from the input data (Sect. 3). The parameterization for the surface albedo α includes exponential aging of snow after a snowfall and an exponential decrease to a constant ice albedo α_{ice} for a thin snowpack (Oerlemans and Knap 1998; Giesen and Oerlemans 2010). The temperature-dependent energy fluxes are represented by a function derived from measurements at weather stations on glaciers in different climates (Giesen and Oerlemans 2012). For air temperatures below a threshold temperature T_{tip} , ψ has a constant (negative) value ψ_{min} . For higher temperatures, ψ increases linearly with T_a , the rate of increase given by b .

Part of the meltwater is allowed to refreeze when a snowpack is present, the refreezing fraction depending on the temperature of the upper 2 m of the glacier (Oerlemans 1991).

2.1.2 Model calibration

The mass balance model is applied to a total of 89 glaciers (Fig. 1). For 72 of these glaciers, winter and annual mass

balance profiles, as well as area-averaged winter and annual mass balance measurements are available from the World Glacier Monitoring Service (WGMS, Zemp et al. 2011, updated; and earlier issues). The winter mass balance profiles were used to determine the vertical gradient of precipitation (Giesen and Oerlemans 2012). Values for the model parameters α_{ice} , ψ_{min} , b and T_{tip} were taken from the AWS measurements in the most similar climate, as described and listed in Giesen and Oerlemans (2012). Generally speaking, there are three parameter sets, for maritime, continental and arctic glaciers (Table 1). The area-averaged winter mass balances were used to calibrate the precipitation from the climate input data (Sect. 3.1) by means of a multiplication factor. Finally, a correction for the air temperature from the climate input data was obtained by minimizing the root-mean-square error of the modelled and measured annual mass balances available for the period 1980–2009.

The set of 72 glaciers mainly consists of glaciers in Scandinavia, European Alps, Western Canada, Caucasus and Central Asia (Table 1). For other glacierized regions of the world, few or no detailed mass balance measurements are available from WGMS. By using less strict selection criteria (for example including glaciers without winter mass balance profiles) and other data sources, we calibrated the mass balance model for 17 additional glaciers in underrepresented regions (Fig. 1). The model parameters for these glaciers were chosen based on values found for glaciers in similar climates and, where necessary, adjusted

to give a satisfactory match with the available mass balance data.

2.2 Volume-area scaling

The initial volume (V) of a glacier is estimated from its reported area (A) using the volume-area scaling relation (Bahr et al. 1997):

$$V = cA^\gamma. \quad (4)$$

Commonly used values for the scaling parameters c and γ are $0.2055 \text{ m}^{3-2\gamma}$ and 1.375 for glaciers and $1.7026 \text{ m}^{3-2\gamma}$ and 1.25 for ice caps (e.g. Radić and Hock 2010; Slangen and van de Wal 2011). These values are mean values from a set of glaciers with known surface area and volume (Chen and Ohmura 1990; Bahr et al. 1997). Several glaciers in the sample are outlet glaciers of ice caps (e.g. Nigardsbreen, Engabreen, Devon Ice Cap) and it is unclear which set of values is most representative in those cases. We use the glacier values for areas smaller than 22.2 km^2 (where the two parameter sets give the same volume) and ice cap values for larger areas. Our simulations start in 1980, but for 59 of the 89 glaciers, no hypsometry is available for this year. In these cases, we use the hypsometry dated closest to 1980 instead.

In addition, Eq. 4 is used to update the glacier area at the end of each year, according to the new glacier volume after accounting for that year's mass balance. The estimated area change is distributed over the glacier hypsometry using

Fig. 1 Location of **a** all glaciers and **b** the 89 modelled glaciers, where the 17 glaciers with limited mass balance information are shown with *open circles*. Glacier locations are from the Randolph Glacier Inventory, version 1 and the World Glacier Inventory for Antarctica

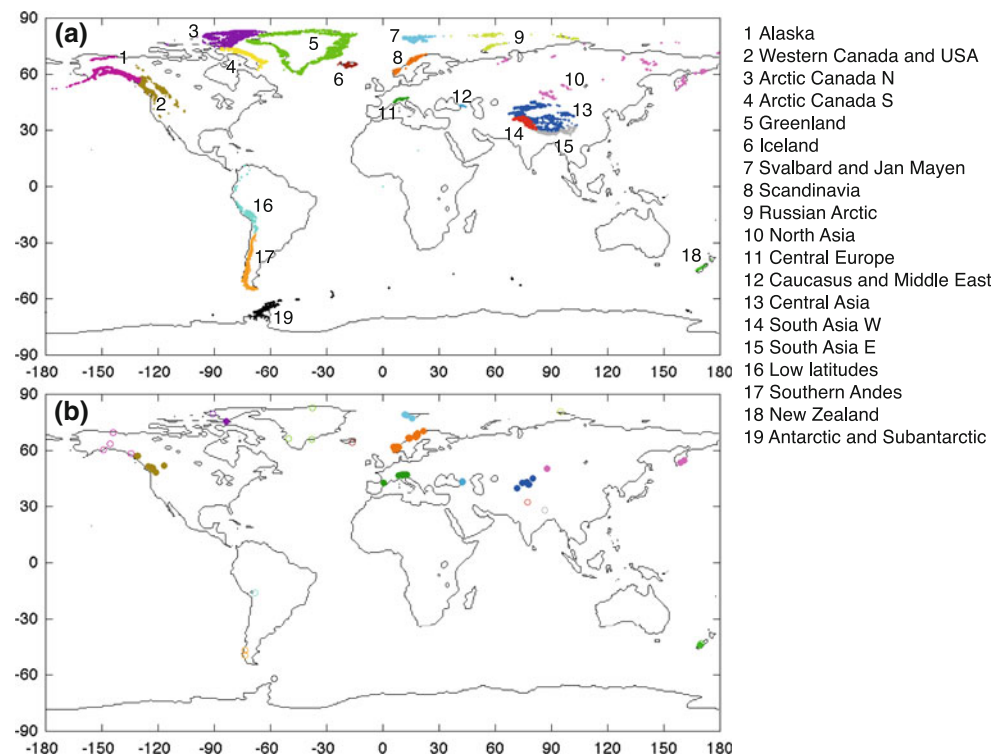


Table 1 Number (#), average number of years with mass balance data and model parameter values for the modelled glaciers in the 19 regions of the Randolph Glacier Inventory

Region	Region name	# Glaciers	# Years	α_{ice}	ψ_{min} (W m ²)	b (W m ⁻² K ⁻¹)	T_{tip} (°C)
1	Alaska	2	30	0.35	-19	8.4	0.2
		1	30	0.35	-26	12.0	4.1
		1	8	0.50	-33	10.8	-0.8
2	Western Canada and USA	13	13	0.35	-26	12.0	4.1
3	Arctic Canada N	2	28	0.50	-33	10.8	-0.8
4	Arctic Canada S	0					
5	Greenland	3	7	0.50	-33	10.8	-0.8
6	Iceland	1	15	0.35	-19	8.4	0.2
7	Svalbard and Jan Mayen	4	25	0.50	-33	10.8	-0.8
8	Scandinavia	25	16	0.35	-19	8.4	0.2
9	Russian Arctic	1	20	0.50	-33	10.8	-0.8
10	North Asia	6	20	0.35	-26	12.0	4.1
11	Central Europe	13	14	0.35	-26	12.0	4.1
12	Caucasus and Middle East	2	26	0.35	-26	12.0	4.1
13	Central Asia	7	12	0.35	-26	12.0	4.1
14	South Asia W	1	8	0.35	-26	12.0	4.1
15	South Asia E	1	4	0.35	-26	12.0	4.1
16	Low latitudes	1	18	0.35	-26	12.0	4.1
17	Southern Andes	2	1	0.35	-19	8.4	0.2
18	New Zealand	2	5	0.35	-19	8.4	0.2
19	Antarctic and Subantarctic	1	5	0.50	-33	10.8	-0.8

functions derived by Huss et al. (2010). They computed normalized ice thickness change per normalized elevation interval from observed surface topography changes on 34 glaciers in Switzerland. Three functions were fitted to the changes observed on small ($A < 5 \text{ km}^2$), middle ($5 < A < 20 \text{ km}^2$) and large ($A > 20 \text{ km}^2$) glaciers. Although these functions give thickness change per elevation interval, we apply them to estimate area change, assuming that thickness changes are accompanied by area changes with a similar distribution over the glacier elevation range. When the predicted area change at a certain altitude is larger than the actual area at that elevation, the remainder is removed from the elevation interval above. Although the majority of the glaciers lose mass in the present and future climate, some glaciers experience periods with mass gain. In that case, the same parameterization is used to distribute the additional area over the glacier elevation range. If the surface area in the lowest elevation bin becomes larger than the average area in the other bins, the surplus area is added to the bin below, allowing the glacier to extend to lower altitudes.

2.3 Upscaling procedure

To obtain regional and global contributions of glaciers to sea-level rise, the simulations for the 89 mass balance

glaciers were used to derive volume projections for all glaciers larger than 0.1 km^2 in the Randolph Glacier Inventory, version 1 (RGI, Arendt and 77 others 2012). This version of the RGI contains individual glacier outlines in some of the regions and outlines of glacier complexes for other regions. Moreover, some ice caps are subdivided into drainage basins while other ice caps are included as one entity. Since there is no consensus whether ice caps should be subdivided and to what level glacier complexes should be separated into tributaries, we did not adjust the outlines given in the RGI. Because Antarctic glaciers were not included in this version of the RGI, we used the glacier locations from the World Glacier Inventory (WGI, World Glacier Monitoring Service (WGMS) 1999, updated 2012). Because the WGI is not complete, we upscaled the inventory using the same method as Radić and Hock (2010). Wherever we mention RGI in this paper, we refer to this combination of RGI and upscaled WGI.

Many RGI glaciers are located in climate model grid cells where none of the modelled glaciers are situated. These glaciers may experience a different change in climate than the 89 mass balance glaciers. We therefore performed additional simulations with the climate anomalies for all grid cells with RGI glaciers. In all simulations for one mass balance glacier, the same set of calibrated model parameters was used.

The normalized volume projections are strongly dependent on glacier size: for the same negative mass balance forcing, small glaciers lose a much larger relative part of their volume than large glaciers. We therefore calculated not only the normalized volume change for the actual size of each mass balance glacier, but also the normalized volume change for a set of glaciers with size $2^{n+1/2}$, for $n = -4$ to 14. We hereby assumed that the shape of the hypsometry is the same for all size classes and simply scaled the hypsometry of each mass balance glacier with a constant factor at all elevations. This is a rather hypothetical assumption, but ensures that the area-averaged mass balance is the same for all size-classes.

For each RGI glacier, the normalized volume change was provided by the simulation for the nearest modelled glacier, with the climate anomalies for the RGI glacier's grid cell and the appropriate size bin. The initial glacier volume of the RGI glacier was multiplied with the obtained normalized volume change and added to the total volume change per region. The regional values were converted to sea-level equivalent (SLE) by assuming an ice density of 900 kg m^{-3} and a commonly used total ocean surface area of $362 \times 10^6 \text{ km}^2$ (Radić and Hock, 2011; Slangen and van de Wal 2011).

3 Meteorological input data

The basis of the meteorological input data is a climatology for the reference period (1980–1999), consisting of the variables air temperature, daily temperature range, precipitation and atmospheric transmissivity. Superimposed on the climatology are monthly anomalies with respect to the reference period for the recent past (1980–2011) and future (2012–2099) climates. We apply absolute differences for air temperature and atmospheric transmissivity and percentual changes for precipitation, while no anomalies are imposed for daily temperature range.

3.1 Climatology (1980–1999)

The air temperature, daily temperature range and precipitation data in the reference climatology are based on the Climate Research Unit (CRU) gridded climatology (CL2.0, New et al. 2002). The CRU CL2.0 data set has a horizontal resolution of $10'$ and provides monthly values of the mean climate over the period 1961–1990 for all grid cells located on land. This data set was chosen for consistency with Giesen and Oerlemans (2012), who calibrated the multiplication factor and vertical gradient of precipitation in the mass balance model using these data.

Since the other climate data sets did not cover the entire period represented by the CRU CL2.0 data, we changed the

reference period to 1980–1999. Monthly mean differences between the periods 1961–1990 and 1980–1999 were calculated from the CRU time series data set (TS3.1, Mitchell and Jones 2005), which has a horizontal resolution of 0.5° . These differences were added to the CRU CL2.0 climate data to obtain a $10'$ monthly climatology for 1980–1999.

For Antarctica, where CRU data are not available, a climatology of monthly air temperatures, daily temperature range and precipitation over the period 1980–1999 was computed from the European Centre for Medium-range Weather Forecasts (ECMWF) ERA-Interim data set. This dataset has a resolution of 0.75° and covers the entire globe (Dee and 35 others 2011).

For all grid cells, the average seasonal cycle in atmospheric transmissivity for the period 1980–1999 was calculated from monthly ERA-Interim values of incoming solar radiation at the surface and at the top of the atmosphere.

3.2 Past climate (1980–2011)

Monthly anomalies of air temperature, precipitation and atmospheric transmissivity were computed from the ERA-Interim data with respect to the reference period 1980–1999. These anomalies were superimposed on the 1980–1999 reference climate (from CRU for air temperature and precipitation and ERA-Interim for atmospheric transmissivity) to provide monthly varying input data to the model for the period 1980–2011.

3.3 Future climate (2012–2099)

For the period 2012–2099, we use monthly anomalies of air temperature, precipitation and atmospheric transmissivity with respect to the reference period 1980–1999, computed for an ensemble of atmosphere-ocean general circulation models (AOGCMs). We selected eight models from the World Climate Research Programme's (WCRP's) Coupled Model Intercomparison Project phase 3 (CMIP3) multi-model dataset (Meehl et al. 2007), forced with the A1B emission scenario (Nakicenovic and 27 others 2000).

The projected summer temperature increase from 1980–1999 to 2080–2099, averaged over all grid cells with RGI glaciers, shows a considerable spread between the eight models (Table 2). Three models give an average temperature increase of 3.7°C , one model projects a temperature increase close to the multi-model mean of 2.9°C , while the other four models range between 2.1 and 2.4°C . Mean winter precipitation is projected to increase in all models, the percentage varying between 12 and 23 %. All models give an average decrease in summer atmospheric transmissivity, most likely due to increased cloudiness. The two GFDL models give a considerably

larger decrease in atmospheric transmissivity than the other six models.

4 Results

4.1 Modelled mass balance

Modelled and measured area-averaged mass balances for the period 1980–2011 for six glaciers in different regions are shown in Fig. 2. The overall correspondence is reasonable, discrepancies are due to shortcomings of the model, but also to the meteorological input data which may not be representative for the local climate at the glacier. For example, the two very wet winters in Norway in 1989 and 1990 are not that extreme in the ERA-Interim data set. Most importantly, the model is able to reproduce the largely varying amplitudes of the interannual variability between the different locations.

A comparison of modelled and measured area-averaged winter and annual mass balance values for all 89 glaciers gives an average linear correlation coefficient r^2 of 0.49 for both winter and annual mass balances. The highest correlation coefficients are obtained for glaciers in maritime regions, where the interannual variations in the mass balance are primarily determined by differences in winter precipitation. Regarding winter mass balances, the performance of our mass balance model is comparable to the models applied by de Woul and Hock (2005) and Rasmussen and Conway (2005). For the matching 52 glaciers over the globe, our mean winter balance r^2 is 0.50, compared with 0.52 by de Woul and Hock (2005). Rasmussen and Conway (2005) obtained an average r^2 value of 0.63 for

12 matching glaciers in Scandinavia, where we have 0.62. For annual mass balances, our linear correlation coefficients are generally lower than in the other two studies, the average r^2 values are 0.66 and 0.53 for the set of 52 glaciers and 0.67 and 0.62 for the 12 Scandinavian glaciers. The lower values obtained with our model possibly result from the temporal resolution of the input data: we use a seasonal cycle based on monthly mean values, while the other two studies use daily meteorological data from weather stations (de Woul and Hock 2005) or an upper-air reanalysis product (Rasmussen and Conway 2005).

The mean modelled annual mass balance over the period 1980–2011 is negative for 78 of the 89 glaciers (Fig. 3), with a median value of -0.38 m w.e. The large positive mass balance values for the two glaciers in New Zealand could not be validated, since mass balance measurements are only available for the last years of the modelled period. Most New Zealand glaciers advanced between 1980 and 2000 (Chinn et al. 2005), at least indicating positive mass balance values.

Figure 3 also shows modelled mass balances for the period 2012–2099 obtained with CGCM3.1(T63) and GFDL-CM2.1 climate data, because upscaled to all glaciers, these simulations result in the highest and lowest estimates of twenty-first century sea-level rise, respectively (Sect. 4.3). The median mass balance for the 89 glaciers over the modelled period is more negative for CGCM3.1 (-1.22 m w.e.) than for GFDL-CM2.1 (-1.03 m w.e.). Future mass balances are not consistently lower for all glaciers with CGCM3.1 climate data. GFDL-CM2.1 projects larger changes in Asia and Central Europe, while future mass balances are more negative for the Arctic regions and the Southern Hemisphere glaciers with the CGCM3.1 climate.

4.2 Future projections for individual glaciers

Future glacier volume simulations for the mass balance glaciers reveal large differences in the glacier response. We discuss the future volume projections for the six glaciers in Fig. 2, obtained with CGCM3.1(T63) and GFDL-CM2.1 climate data (Fig. 4).

The future glacier changes are primarily dictated by the projected increases in temperature, resulting in net volume loss for all six glaciers. There are large differences between the future projections obtained with the two climate models, even though they use the same future emission scenario. Although GFDL-CM2.1 climate results in a smaller global volume reduction (Sect. 4.3), Djankuat Glacier and Maliy Aktru disappear faster than with CGCM3.1 input data. Differences are small for Jamtalferner, while CGCM3.1 gives a larger volume reduction for the Arctic glaciers.

Table 2 CMIP3 models used in this study and the change in summer air temperature (ΔT_s), winter precipitation (ΔP_w) and summer atmospheric transmissivity ($\Delta \tau_s$) between 1980–1999 and 2080–2099, averaged over all grid cells with RGI glaciers and weighted by the glacier area. Summer is defined as the period April–September on the Northern Hemisphere and October–March on the Southern Hemisphere, the winter period covers the remaining 6 months of the year

Model	Country	ΔT_s (°C)	ΔP_w (%)	$\Delta \tau_s$
CGCM3.1(T63)	Canada	3.7	20	−0.028
CNRM-CM3	France	2.4	14	−0.023
CSIRO-Mk3.0	Australia	2.2	14	−0.028
ECHAM5/MPI-OM	Germany	3.7	15	−0.031
GFDL-CM2.0	USA	3.0	19	−0.057
GFDL-CM2.1	USA	2.3	14	−0.043
NCAR-PCM	USA	2.1	12	−0.021
UKMO-HadCM3	UK	3.7	23	−0.032
AOGCM mean		2.9	16	−0.033

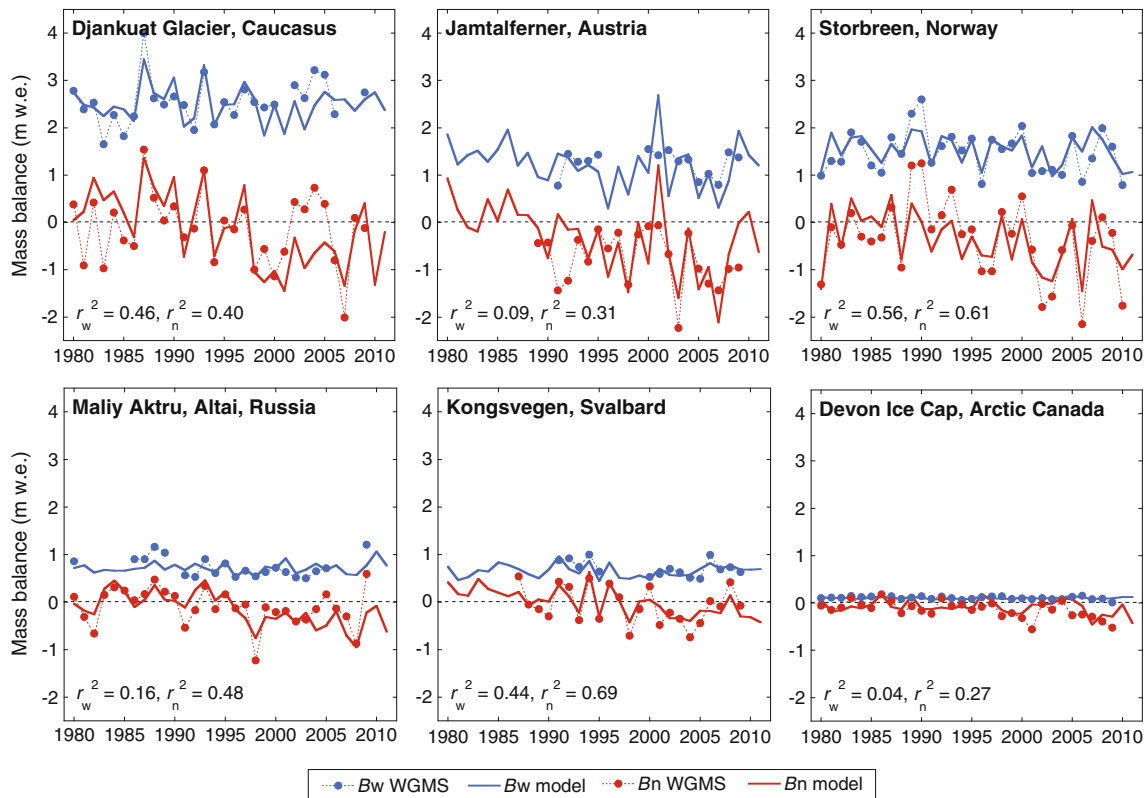
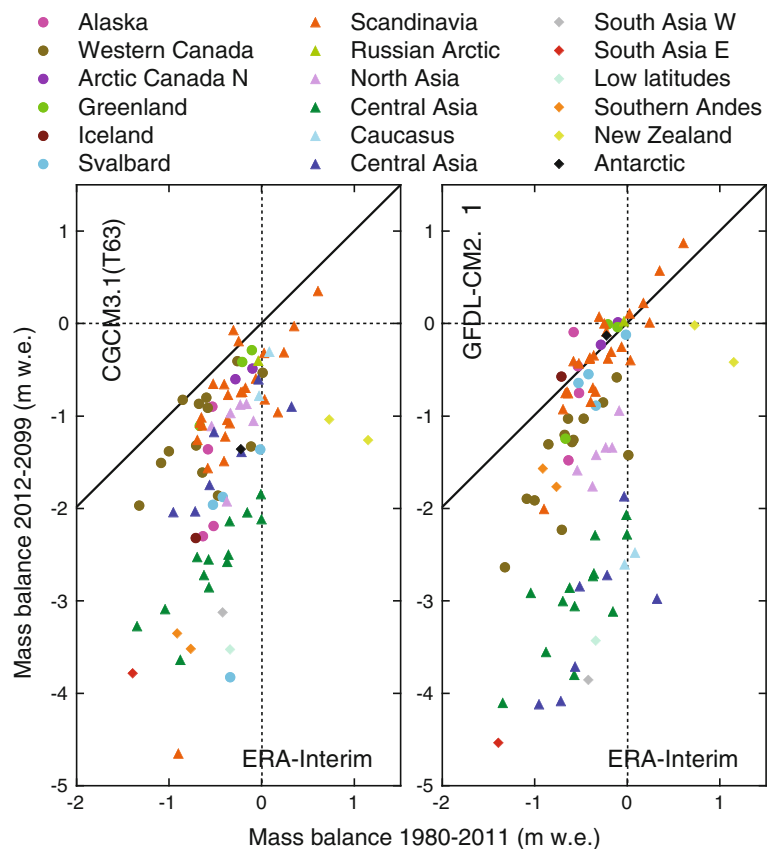


Fig. 2 Modelled and measured area-averaged winter (B_w) and annual (B_n) mass balance for six glaciers in different climatic regions. The linear correlation coefficient between modelled and measured winter (r_w^2) and annual (r_n^2) mass balance is given in the lower left corner of each panel

Fig. 3 Mean annual mass balance (B_n) over the period 2012–2099 for the 89 glaciers modelled with the CGCM3.1(T63) and GFDL-CM2.1 climate, versus mean B_n for the period 1980–2011, modelled with ERA-Interim input data. The mass balance values were calculated for a non-changing surface area



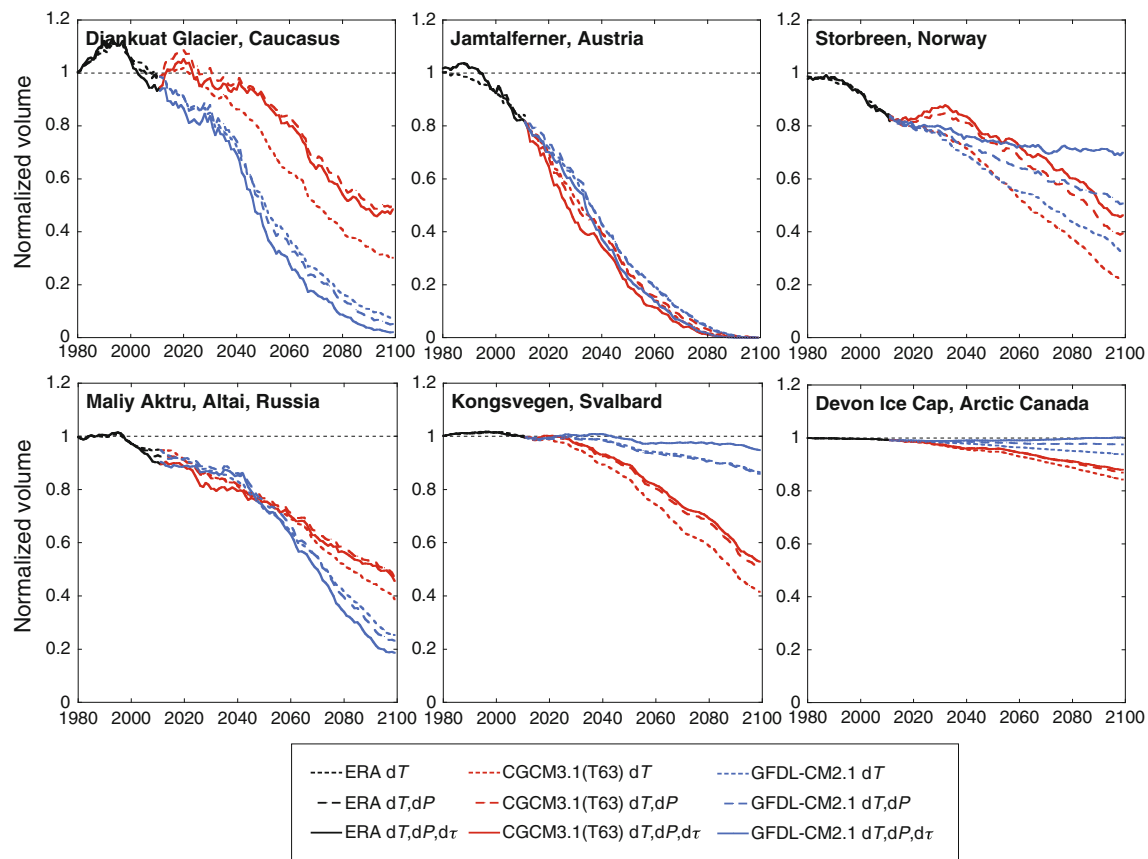


Fig. 4 Glacier volume projections with ERA-Interim for the period 1980–2011 and CGCM3.1(T63) and GFDL-CM2.1 for the period 2012–2099 for six glaciers in different climatic regions. Projections

Increases in precipitation have a considerable compensating effect on the mass balance for maritime glaciers in the sample, like Storbreen. Changes in atmospheric transmissivity are too small in CGCM3.1 to significantly affect the mass balance. For GFDL-CM2.1, the anomalies are generally larger. For Scandinavia and the Arctic, the lower atmospheric transmissivity, together with increased precipitation almost or entirely compensates for the effect of the increase in temperature.

4.3 Regional and global volume change

The upscaled volume projections indicate that the largest contributions to sea-level rise in the past 30 years originated from the peripheral glaciers of Greenland and Antarctica and the glaciers in Alaska and Central Asia (Fig. 5a). The estimated total contribution of glaciers to sea-level rise over the period 1980–2011 is 0.022 m (Table 3).

Averaged over the eight climate models, the glacier contribution to sea-level rise for 2012–2100 is estimated at 0.102 ± 0.028 m (multi-model mean and standard deviation, Table 3), with a minimum of 0.065 m (GFDL-CM2.1)

are shown for simulations with only temperature changes (dT), temperature and precipitation changes ($dT + dP$) and with additional changes in atmospheric transmissivity ($dT + dP + d\tau$)

and a maximum of 0.146 (CGCM3.1(T63)). The AOGCM simulations indicate that the glaciers in the Antarctic, Alaska, Central Asia and Greenland will remain the largest contributors to sea-level rise in the twenty-first century, together accounting for 65 ± 4 % of the total projected sea-level rise.

Not only the total sea-level contribution varies by a factor of two, the relative contributions by the glaciers in the 19 regions are also very different for the eight climate models (Fig. 5c). The only two AOGCMs that give similar values for the total and regional sea-level contributions, are UKMO-HadCM3 and ECHAM5/MPI-OM. The large difference in the global sea-level contribution between CGCM3.1 and GFDL-CM2.1 mainly results from highly different contributions from the Antarctic glaciers (Fig. 6). Especially at the higher Northern Hemisphere latitudes, the variation in the sea-level contribution from the different climate models is large, with values up to 0.01 m difference from the multi-model mean.

Regarding relative volume loss, the largest changes are expected to occur in Central Europe, South Asia East and Caucasus/Middle East, where more than 70 % of the 2011 ice volume is projected to be lost by 2100 (Table 3).

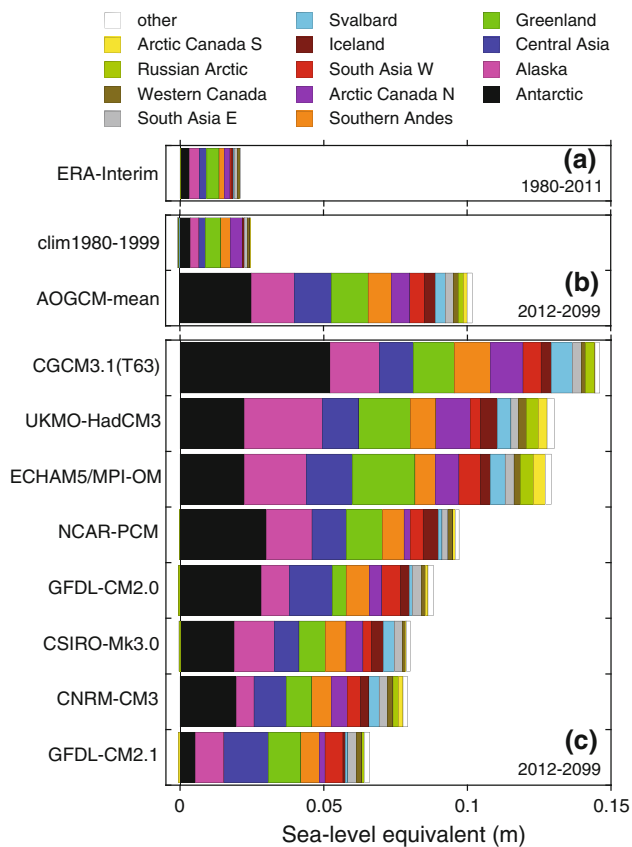


Fig. 5 Regional contributions to sea-level rise for **a** 1980–2011 with ERA-Interim, **b** 2012–2099 with the 1980–1999 climate and the mean of the projections with AOGCM input data and **c** 2012–2099 with climate data from the eight individual AOGCMs. The contributions from Scandinavia, Central Europe, Caucasus, North Asia, New Zealand and the low latitudes were too small to be shown individually and were combined into ‘other’

Averaged over all regions and climate models, 18 ± 5 % of the 2011 glacier volume and 21 ± 5 % of the 1980 glacier volume is projected to be lost by the end of the twenty-first century.

If the reference climate (the mean over 1980–1999) is extended into the future without applying any additional forcing after 2011, another 0.024 m of SLE is lost by 2100 (Fig. 5b). The glaciers are projected not to have reached an equilibrium with the climate forcing in 2100, indicating that even without future climate change, the global glacier volume would reduce in the twenty-first century and beyond.

4.4 Regional 21st century climate change

To improve our understanding of the large spread in global and regional sea-level contributions modelled with climate data from the eight climate models, we calculated regional values of the change in summer air temperature (T_s), winter

Table 3 Total area A (km²) and volume V (km³) in 1980 of the modelled RGI glaciers in the 19 regions, the multi-model mean change in volume ΔV (%) and the corresponding sea-level equivalent SLE ($\times 10^{-3}$ m) over the periods 1980–2011 and 2012–2099

Region	A	V	ΔV 1980–2011	SLE 1980–2011	ΔV 2012–2099	SLE 2012–2099
Alaska	87,705	19,066	−7.4	3.5	−34.6	15.2
Western Canada and USA	14,312	1,868	−14.2	0.7	−44.7	1.8
Arctic Canada North	113,710	32,597	−2.4	2.0	−8.1	6.5
Arctic Canada South	40,571	13,380	−0.9	0.3	−4.0	1.3
Greenland	123,260	49,766	−3.5	4.4	−10.5	12.6
Iceland	11,123	4,896	−5.1	0.6	−32.0	3.7
Svalbard and Jan Mayen	33,552	6,579	−1.0	0.2	−21.5	3.5
Scandinavia	2,832	372	−4.7	0.0	−28.4	0.3
Russian Arctic	51,357	20,582	0.2	−0.1	−3.3	1.8
North Asia	2,770	246	−8.2	0.1	−40.9	0.2
Central Europe	1,971	134	−16.4	0.1	−87.5	0.3
Caucasus and Middle East	1,095	69	−4.1	0.0	−73.3	0.1
Central Asia	67,446	10,716	−11.0	2.9	−54.2	12.9
South Asia West	33,555	3,706	−7.9	0.7	−61.3	5.2
South Asia East	21,704	1,759	−26.9	1.2	−88.4	2.8
Low latitudes	4,944	589	−7.3	0.1	−65.6	0.9
Southern Andes	33,709	12,666	−6.1	1.9	−27.2	8.1
New Zealand	1,076	115	13.9	−0.0	−4.6	0.0
Antarctic and Subantarctic	168,160	56,759	−2.3	3.2	−18.0	24.9
Total	814,852	235,866	−3.7	21.7	−18.0	101.8

precipitation (P_w) and summer atmospheric transmissivity (τ_s) for the eight AOGCMs. The regional averages are weighted by the glacier area in each climate data grid cell. The summer half year covers the months April–September in the Northern Hemisphere (NH) and October–March in the Southern Hemisphere (SH), the remaining 6 months represent the winter half year. Although some glaciers receive the majority of the accumulation in summer or experience considerable melt in winter, the winter and summer seasons correspond to the main accumulation and ablation seasons on the majority of the glaciers. While modelled changes in T_s , P_w and τ_s exhibit large variability within the regions (Fig. 7), some general patterns can be discerned.

For the majority of the regions in the NH, projected summer warming varies around the all-region mean value of 2.9 °C. The temperature change is approximately 1 °C higher for the regions in Asia and 1 °C lower for the regions in the SH.

Projected changes in winter precipitation for the eight climate models are less variable in Asia and the SH than at higher latitudes in the NH, where P_w increases are generally larger. Precipitation changes in Arctic Canada North

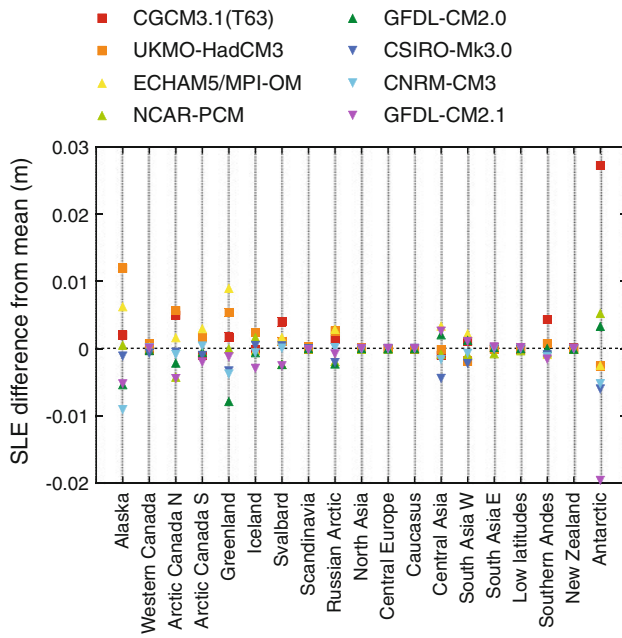


Fig. 6 Difference in regional contributions to sea-level rise with input data from the eight AOGCMs with respect to the multi-model mean over 2012–2099

and the Russian Arctic are well above the all-region mean in all models.

Summer atmospheric transmissivity is projected to decrease at the higher latitudes in the NH and for the Antarctic, while changes are small in Asia and the other regions in the SH. All models agree on an increase in τ_s for Central Europe and Caucasus.

Although the largest global sea-level contribution is obtained with input data from CGCM3.1(T63), UKMO-HadCM3 shows the largest summer temperature increases in most of the regions. This model also has the highest increases in winter precipitation in many regions, which together with large decreases in τ_s partly compensate for the high summer temperatures. CGCM3.1 temperature changes in the SH considerably exceed those in the other models, especially for the Antarctic, explaining the large projected sea-level contribution for this region. GFDL-CM2.1 is the coldest model for some of the regions with large ice volumes, like Greenland and the Antarctic. Furthermore, it projects a large increase in P_w and a considerable lowering of τ_s in other important regions, like Alaska and Arctic Canada.

4.5 The effect of changes in precipitation and atmospheric transmissivity

The large differences in the projected sea-level contribution between the eight climate models suggest that changes in precipitation and atmospheric transmissivity play a significant role in the glacier response to future climate

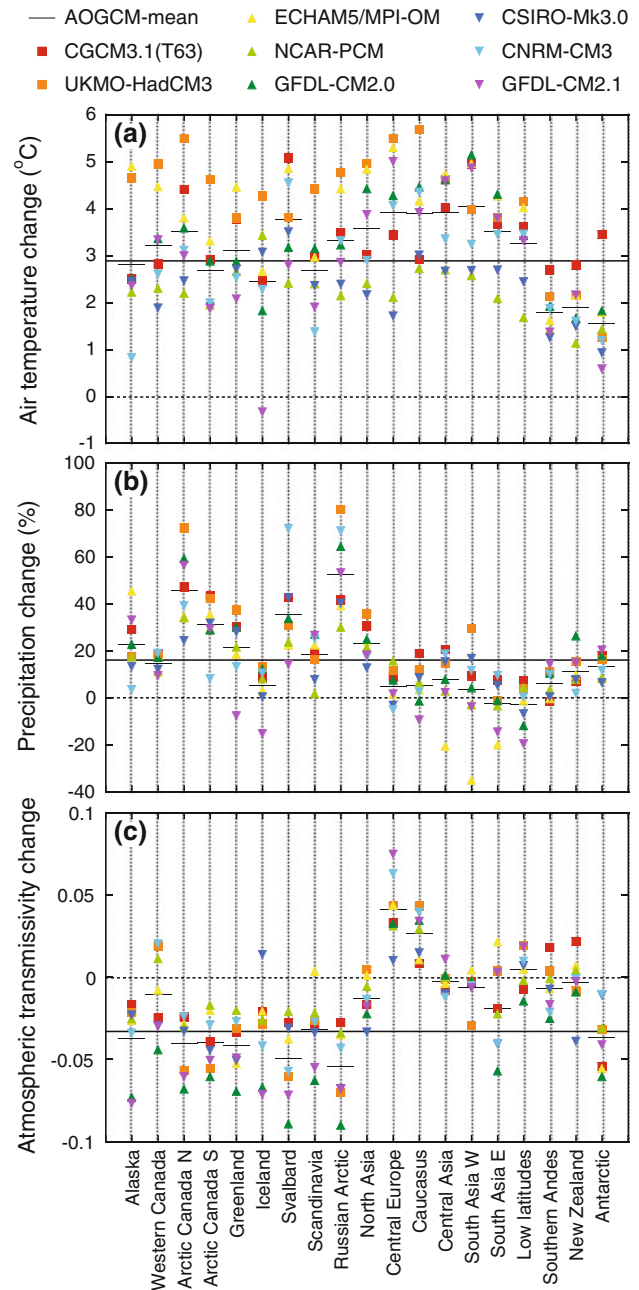


Fig. 7 Regional projected changes in **a** summer air temperature, **b** winter precipitation and **c** summer atmospheric transmissivity between 1980–1999 and 2080–2099 for the eight AOGCMs. The solid horizontal line indicates the mean value over all regions, weighted with the glacier area, as presented in Table 2

change. To examine this effect in more detail, we computed the global and regional sea-level contributions with input data from the eight AOGCMs, for a case with only temperature changes (dT) and a case with changes in air temperature and precipitation, but not in τ ($dT + dP$).

When changes in τ are not taken into account, the global contribution to sea-level rise increases by 0.016 ± 0.007 m (17 ± 5 %) on average, with the largest increase

in the contribution by the two GFDL models (Fig. 8). When anomalies in precipitation are also excluded, hence with only anomalies in temperature, the mean sea-level contribution increases further by 0.020 ± 0.005 m (0.035 ± 0.011 m (35 ± 17 %) higher than with all anomalies included). For ECHAM5/MPI-OM, the additional change is small, which is probably related to reduced volume change in Asia, where precipitation is projected to decrease considerably in this model (Fig. 7).

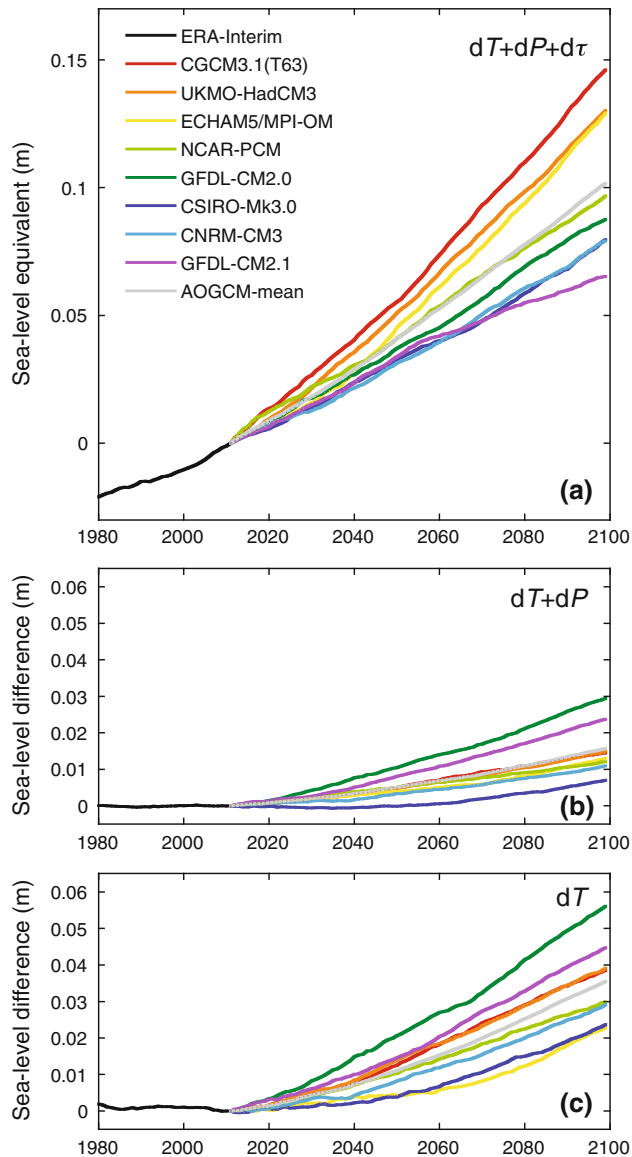


Fig. 8 Projected global glacier volume change (in SLE) with ERA-Interim for the period 1980–2011 and eight AOGCMs for the period 2012–2099, with **a** anomalies in air temperature, precipitation and atmospheric transmissivity ($dT + dP + d\tau$), **b** anomalies in air temperature and precipitation ($dT + dP$) and **c** only anomalies in air temperature (dT). Panels **b** and **c** show the SLE difference with regard to the curves shown in **a**; note the different vertical scale

The multi-model mean regional changes in the sea-level contribution when anomalies in precipitation and atmospheric transmissivity are excluded, are illustrated in Fig. 9a. For all regions, the glacier volume change is largest when only temperature anomalies are taken into account. Both changes in P and τ have a considerable compensating effect on the volume changes imposed by future warming. Since the projected anomalies in P and τ are largest for the Arctic regions (Fig. 7), the total sea-level

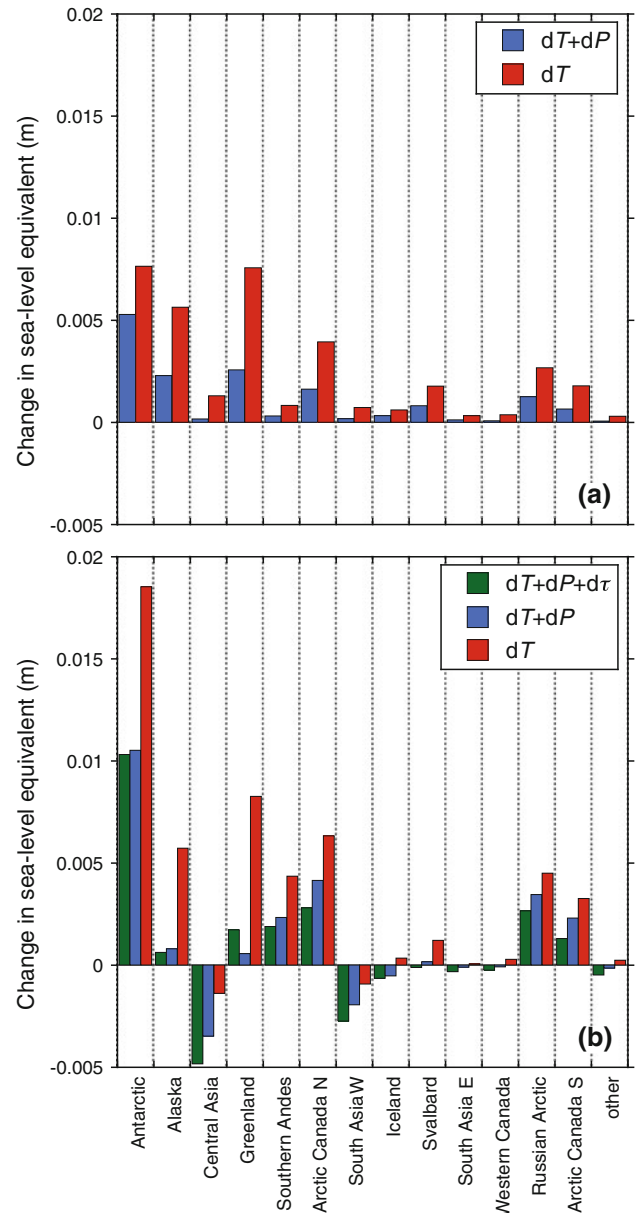


Fig. 9 Difference between the AOGCM mean regional glacier volume projections (in SLE) for the period 2012–2099 with all anomalies included and with **a** only anomalies in air temperature (and precipitation), **b** globally uniform anomalies in air temperature, precipitation and atmospheric transmissivity

contribution from these regions increases substantially when anomalies in P and τ are excluded.

As a final experiment, we applied a globally uniform change in climate, with linear changes in T , P and τ between 1980–1999 and 2080–2099, the values given by the mean change over all regions and models (Table 2). Summed over all regions, the sea-level contribution increases by 0.012 m when anomalies in T , P and τ are imposed, and by 0.051 m when only air temperature uniformly increases by 2.9 °C. Major negative changes occur in Asia, where the projected increase in air temperature is larger than the all-region mean, while the increase in precipitation and the decrease in atmospheric transmissivity are smaller than the average. The largest increase in the sea-level contribution is found for the Antarctic, mainly because the temperature anomaly becomes much larger than projected by most climate models. Again, not only anomalies in air temperature result in large changes in the sea-level contribution, anomalies in precipitation and atmospheric transmissivity also have a considerable effect on glacier volume changes.

5 Discussion

5.1 Model uncertainty

This paper discussed the uncertainty in the future sea-level contribution from glaciers introduced by differences in the future climate projected by eight climate models. Apart from this uncertainty, there are several simplifications and assumptions in our approach that also result in uncertainties in the modelled global sea-level contribution. In this section, we quantify the uncertainties that can be addressed with the model and discuss the major other sources of uncertainty.

5.1.1 Model calibration

The mass balance model is calibrated with available mass balance measurements for 89 glaciers in different climatic regions. In the last step of the calibration procedure, modelled and measured annual mass balance are matched by applying a correction to the air temperature. In the case of changes in the climate input data, the model parameters or the glacier hypsometry, the model needs to be recalibrated. Since the temperature correction is always tuned to match the measured mass balance, the effect of a recalibration procedure on the volume projections is small. However, uncertainties in the mass balance records and the calibration method may affect the results. We estimate this effect by increasing the temperature correction by 0.5 °C,

roughly corresponding with a mass balance error between 0.1 m w.e. on cold and dry glaciers and 0.5 m w.e. on maritime glaciers. This results in a change in the simulated sea-level contribution by +0.017 m for 1980–2011 and +0.024 m for 2012–2099.

5.1.2 Upscaling

The model is applied to 89 glaciers with available mass balance measurements, after which the simulated volume changes are upscaled to all glaciers outside the Greenland and Antarctic ice sheets. Hereby we assume that the mass balance of each modelled glacier is representative for the surrounding RGI glaciers, while accounting for the dependency of normalized volume change on glacier size and the actual climate change at the RGI glacier's grid cell. The validity of this assumption and its associated uncertainty were estimated by applying the upscaling method to the set of 89 glaciers. Hence, the normalized volume change of each of the 89 glaciers was simulated with the mass balance calculated for the nearest of the remaining 88 glaciers. For the six glaciers discussed before, we illustrate the volume change obtained with the original and the validation method (Fig. 10). For Kongsvegen and Devon Ice Cap, where the validation glacier is much smaller than the actual glacier, the volume decreases more rapidly in the validation run. However, this is not a systematic feature in the total set of 89 glaciers. For the other four glaciers, the change in the multi-model mean volume change is smaller than the range in the model ensemble, although for the individual climate model runs, the differences can be larger. The mean change in the 1980–2099 normalized volume loss for the sample of 89 glaciers is close to zero (0.17 %), with a standard deviation of 18.1 %.

If the volume change of the second nearest glacier is used in the upscaling to all RGI glaciers larger than 0.1 km², changes in the global sea-level contribution are small: −0.001 m for the period 1980–2011 and −0.003 m for the period 2012–2099. Differences in the projected volume change for individual glaciers and regions cancel in the total. The largest twenty-first century multi-model mean change in the sea-level contribution is obtained for the Antarctic (−0.006 m), followed by the Russian Arctic (+0.002 m); for the other regions the differences are smaller than 0.001 m. The large sensitivity for the Antarctic is a result of the relatively large glacier area and volume in this region, but also of the climatic difference between the one modelled glacier and the nearest glacier in the Southern Andes.

In general, the sea-level contribution for regions with only one modelled glacier and limited mass balance information is more uncertain than for regions with better data coverage. We assume that the standard deviation of

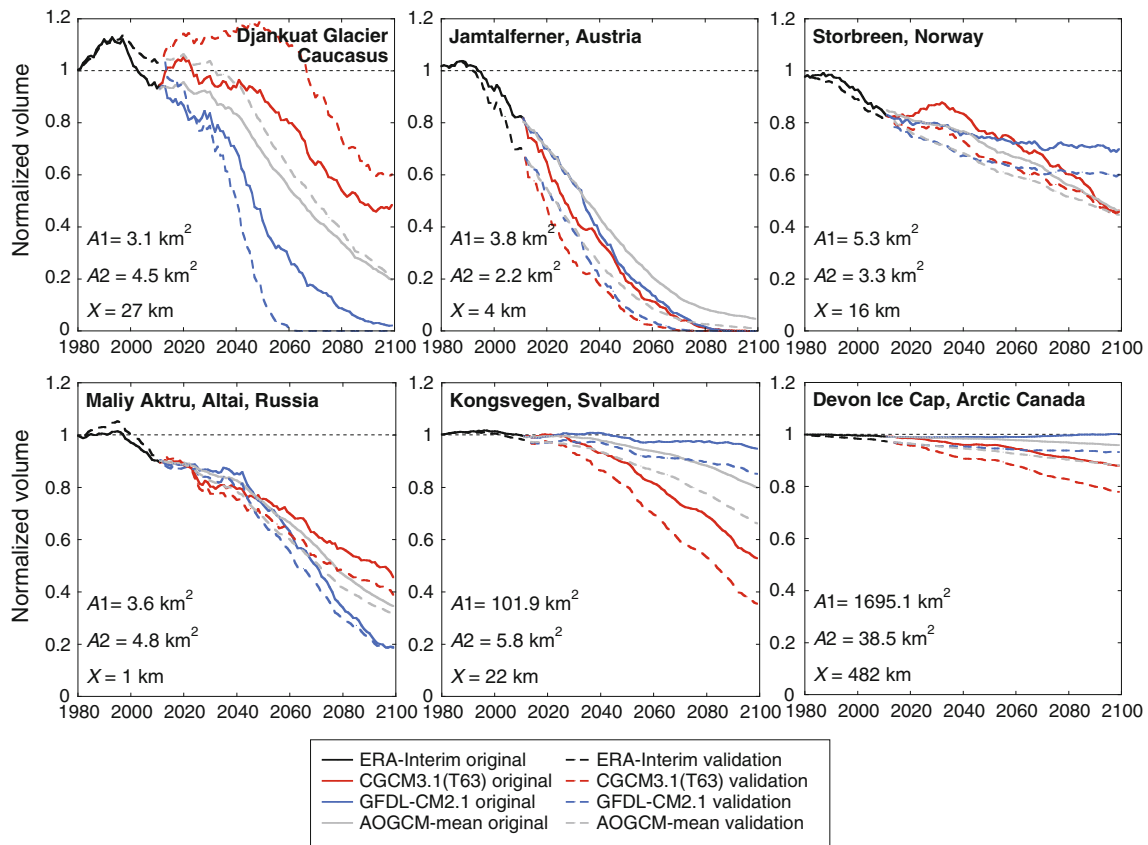


Fig. 10 Glacier volume projections with ERA-Interim for the period 1980–2011 and CGCM3.1(T63), GFDL-CM2.1 and the AOGCM-mean for the period 2012–2099 for six glaciers in different climatic regions. Projections are shown for the original simulation and for a

validation experiment where the volume change was derived from the nearest of the 88 other modelled glaciers. The areas of the modelled glacier (A1) and the nearest glacier (A2), as well as the distance between the two glaciers (X) are given in each panel

the validation test for the 89 glaciers is a good measure for the uncertainty in the upscaling method. Applying the 18.1 % uncertainty to the global sea-level contributions, this amounts to 0.004 m for the period 1980–2011 and 0.018 m for 2012–2099.

5.1.3 Constant model parameters

In addition to the applied changes in air temperature, precipitation and atmospheric transmissivity, model parameters that are assumed to remain constant in the simulations may change in the future climate.

Reduced snowfall and increased dust supply from the surroundings could result in a lowering of the surface albedo, especially of ice (e.g. Oerlemans et al. 2009). A linear reduction of the ice albedo by 0.1 over 100 years increases the multi-model mean global sea-level contribution by 0.009 m.

Furthermore, the parameters defining the temperature-dependent flux may be different in the changed climate, due to changes in cloudiness, humidity and wind speed.

The effect of changes in cloud cover are taken into account in the net solar radiation contribution, by using a variable atmospheric transmissivity. Cloudiness changes will also affect the incoming longwave radiation, but since this flux is not calculated explicitly in the model, this effect cannot be quantified. Part of the increase in incoming longwave radiation for increasing cloud cover may already be included due to the associated increase in air temperature. The sensitivity of the future volume projections to changes in the temperature-dependent flux parameters is estimated by increasing b by $0.02 \text{ W m}^{-2} \text{ K}^{-1}$ and ψ_{\min} by 0.1 W m^{-2} per year from 2012 onwards. The change in b and ψ_{\min} over 100 years roughly corresponds to the range in values determined for glaciers within similar climates (Giesen and Oerlemans 2012). This results in a multi-model mean increase in the sea-level contribution of 0.031 m. This value is larger than the effect of changes in atmospheric transmissivity on the sea-level contribution (-0.016 m , Sect. 4.5), implying that future changes in the temperature-dependent fluxes could compensate the changes in net solar radiation.

5.1.4 Glacier inventory

In this study, we use the glacier area reported in the RGI as the initial glacier area in 1980. However, the glacier area information in the RGI is a compilation of area measurements by many different investigators, with different techniques and covering different time periods. Furthermore, the disappearance of the part of tidewater glaciers that is currently below sea level will not contribute to sea-level rise, which is not taken into account in this study. These shortcomings are addressed by assuming an uncertainty in the glacier area of $\pm 10\%$, which results in a change in the sea-level contribution of ± 0.006 m for 1980–2011 and ± 0.011 m for the period 2012–2099 (multi-model mean).

In addition, some RGI glaciers and ice caps are subdivided into smaller entities, while others are not. It is unknown until which level glaciers and ice caps have to be subdivided to obtain optimal results from volume-area scaling. However, the choice of outlines will affect the total volume contained in glaciers and possibly the projected volume change. To arrive at a first estimate of this uncertainty, we subdivided all glaciers larger than 50 km^2 into ten equally sized glaciers. This has a large effect on the total volume contained in glaciers, which is reduced by 41 %. Since the initial surface area and hence mass balance are unchanged, the change in projected sea-level rise is smaller (-0.001 m for 1980–2011 and -0.029 m or 26 % for 2012–2099).

Glacier outlines for Antarctica were not included in version 1 of the RGI and we used upscaled data from the WGI instead. A recent, complete inventory of the Antarctic peripheral glaciers estimates the total area of glaciers larger than 0.1 km^2 at $132,837 \text{ km}^2$ (Bliss et al. 2013), which is 79 % of the area we used. Using our volume-area scaling method, the total volume for the new inventory amounts to $42,146 \text{ km}^3$, which is 74 % of our volume. The inventory by Bliss et al. (2013) contains a larger number of glaciers surrounding the entire continent, while we only have glaciers at the Antarctic Peninsula. With this new inventory, our simulated sea-level contributions from Antarctic glaciers become 0.001 and 0.007 m larger for 1980–2011 and 2012–2099, respectively. Together with the limited mass balance measurements for this region, this makes our volume projections for Antarctic glaciers highly uncertain.

5.1.5 Volume-area scaling

The scaling parameters in the volume-area scaling relation have been derived for a relatively small number of glaciers. While the values for γ are based on both theory and observations, the values of c vary considerably within the set of glaciers. This implies that applying the volume-area

scaling relation with a constant value of c may give large errors when the set of glaciers is small; for a large sample under- and overestimated volumes are expected to compensate each other when an average value for c is used. While we do not apply the volume-area scaling relationship to each RGI glacier individually, the effect of volume change on the surface area is calculated separately for all 19 size classes of each of the 89 calibrated glaciers. Secondly, we used the ice cap parameters to all glaciers larger than 22.2 km^2 , which may include several large glaciers that are better represented by the glacier parameters. Finally, the values for the scaling parameters were derived from area and volume information of glaciers that were close to equilibrium with the present-day climate. These values may no longer be valid for the future, when many glaciers are far out of equilibrium with the warming climate. Already, some rapidly shrinking glaciers are wasting away and do no longer display healthy glacier dynamics (e.g. Paul et al. 2004; Peltó 2006). Since there is no information on variation of the scaling parameters in time, we do not address this potential error source. We estimated the uncertainty resulting from using a relatively small sample of glaciers with unknown c -values by varying c by its standard deviation, which is approximately one third of the mean value (Bahr 1997). This affects the multi-model mean sea-level contribution for 1980–2011 by ± 0.001 m and the 2012–2099 value by ± 0.015 m. By comparison, when the glacier parameters are used for all glaciers, the sea-level change over the period 2012–2099 increases by 0.014 m.

5.1.6 Combined uncertainty estimate

Assuming that all calculated uncertainties are independent, we arrive at a combined uncertainty estimate over the period 1980–2011 of ± 0.019 m. For the period 2012–2099, the uncertainty amounts to ± 0.057 m, twice as large as the standard deviation of the ensemble of AOGCM runs (0.028 m). Including this standard deviation as the uncertainty in the future climate, the uncertainty estimate for the future projections becomes ± 0.063 m. This is 62 % of the multi-model mean projected sea-level rise.

5.1.7 Other sources of uncertainty

Other uncertainties that cannot be addressed by the model are associated with processes that are not included in the model and would require a more sophisticated glacier model. We do not take into account the effect of debris cover on the glacier mass balance, since debris cover is highly spatially variable and its effect on the mass balance is still poorly understood (Mihalcea et al. 2008; Scherler et al. 2011). Volume-area scaling gives an instantaneous

response of the area to changes in the mass balance, while especially for larger glaciers, this response may be delayed by years to decades. An unrealistically fast retreat of the terminus to higher elevations has a positive effect on the mass balance and may lead to an underestimation of the volume change. To obtain a more realistic glacier response, a dynamical glacier model should be used instead of volume-area scaling. Such a model would additionally include the positive feedback between mass balance and elevation changes, which is not included in our approach, but can be important in the response of ice caps with a small elevation range (Giesen and Oerlemans 2010). However, dynamical glacier models require information on the glacier surface and bed geometry, which is generally not available. Furthermore, we only address the changes in the surface mass balance, not in the total glacier mass balance, which also include mass changes by basal melting and, for glaciers that terminate in water, frontal melting and calving. Frontal melting will likely increase when water temperatures rise in a warming climate. Frontal melting and calving will no longer contribute to the mass balance when the glacier retreats out of the water, but may become an important term for other glaciers where a frontal lake is formed during the glacier retreat. Additionally, the coarse resolution of the climate models may result in climate projections for the glacierized regions that may not be representative of the real changes in the local glacier climate. These uncertainties also cannot be addressed in this study. Using input climate data from RCMs could improve the regional projections, but especially in regions with rugged topography the climate in the glacier valleys will still not be resolved.

5.2 Comparison to other studies

A comparison of our estimated recent (1980–2011) volume loss from glaciers with values from other studies is complicated by the different regions and time periods considered. Our global value (0.022 ± 0.019 m) for the period 1980–2011 is generally lower than values reported from other studies. For example, our value is 75 and 81 % of the estimates from the modelling studies by Slangen et al. (2012) and Marzeion et al. (2012), respectively. Compared to studies that use upscaling of mass balance measurements, our estimate is not very different from the value given by Dyurgerov (2010) (84 %), but only slightly more than half the value from Cogley (2009b) (57 %). These lower values could be an indication of a too low model sensitivity to climate changes or of a non-representative set of modelled glaciers for global upscaling. The differences could also be a result of an erroneous initial imbalance in some of the regions. Our sea-level contribution for the last decade excluding the glaciers around the Greenland and Antarctic ice sheets is 56 % larger than the estimate from

Jacob et al. (2012), who use mass change rates from the Gravity Recovery and Climate Experiment (GRACE) satellite mission. Especially for Central and South Asia, where Jacob et al. (2012) find relatively small changes, our values are higher. Since the GRACE estimates include mass loss by calving, which is expected to have increased over the past decade, this positive difference is hard to explain. Although the differences between the studies are large, all estimates fall within our uncertainty range.

The global twenty-first century contribution of glaciers to sea-level rise found in this study is smaller, but falls within the uncertainty ranges of the values found in two other studies (Table 4). Like in this study, Radić and Hock (2011) and Slangen et al. (2012) use a multi-model ensemble with the A1B emission scenario, although the number and choice of models is different in the three studies. Radić and Hock (2011) (RH11) apply a positive degree-day model, calibrated for 36 glaciers, to all glaciers in the extended World Glacier Inventory (WGI-XF, Cogley 2009a), after which the results are upscaled for regions where this inventory is not complete. Slangen et al. (2012)

Table 4 Projected sea-level equivalent SLE ($\times 10^{-3}$ m) for this study over the period 2000–2099, from Radić and Hock (2011) for the period 2001–2100 (RH11) and from Slangen et al. (2012) for the period 2000–2099 (S12)

Region	This study	RH11	S12
Alaska	17.0	25.7	27.2
Western Canada and USA	2.0	2.4	3.9
Arctic Canada North	7.3	27.0	31.2
Arctic Canada South	1.5		
Greenland	14.9	3.6	8.3
Iceland	4.0	4.4	3.3
Svalbard and Jan Mayen	3.7	13.9	7.8
Scandinavia	0.3	0.2	0.5
Russian Arctic	1.6	13.3	10.6
North Asia	0.3	0.1	0.4
Central Europe	0.3	0.4	0.5
Caucasus and Middle East	0.1	0.1	0.2
Central Asia	14.2		
South Asia West	5.8	3.3	19.6
South Asia East	3.3		
Low latitudes	1.0	0.2	0.9
Southern Andes	8.5	7.4	10.7
New Zealand	0.0	0.1	0.2
Antarctic and Subantarctic	26.2	21.8	34.3
Total	112	124	159
Uncertainty	± 63	± 37	± 52

In the two previous studies, Arctic Canada N and S form the region Arctic Canada and Central Asia, South Asia W and E form the region High Mountain Asia; one value is given for each combined region

(S12) calculate volume changes for all glaciers in WGI-XF from location-dependent mass balance sensitivities and subsequently scale the results to obtain regional and global contributions to sea-level rise. In both studies, volume-area(-length) scaling is used to incorporate changes in glacier area.

Looking at regional values, RH11 and S12 both find considerably higher contributions from Alaska and the Arctic regions than this study. This could be due to the lower sensitivity of our model to temperature changes and the higher sensitivity to precipitation changes compared to RH11 (Giesen and Oerlemans 2012) and to the large effect of changes in atmospheric transmissivity in these regions. A better understanding of the impact of atmospheric transmissivity changes can be obtained from more detailed surface energy balance modelling, our results indicate that this is especially important for glaciers in the Arctic regions. The higher contribution of glaciers in Greenland in this study mainly results from the total glacier area that is a factor 2.25 larger in the RGI compared to the upscaled WGI-XF (Radić and Hock 2010). RH11 report a seven times smaller volume change for glaciers in Central and South Asia, which could be related to the small number of mass balance observations for South Asia. Some of the differences between the three studies could also be due to the different climate model ensembles used.

This study provides a first attempt to address the effect of changes in climate variables other than air temperature and precipitation on glacier volume projections. We find that the projected general decrease in atmospheric transmissivity has a non-negligible effect on the net solar radiation. However, we cannot quantify simultaneous changes in other energy fluxes, primarily net longwave radiation. Because of the different methods used, our future projections complement existing studies. The results demonstrate that including changes in additional climate variables is important for improved understanding of future glacier changes.

6 Conclusions

We applied a surface mass balance model to 89 glaciers in different climatic regions, after which the resulting glacier volume changes were scaled to obtain global glacier volume projections for the period 1980–2099. The recent (1980–2011) sea-level contribution from glaciers is estimated at 0.022 ± 0.019 m. The multi-model ensemble mean future sea-level rise (2012–2099), obtained from simulations with climate input data from eight AOGCMs, is 0.102 ± 0.063 m. This is 18 ± 11 % of the estimated total volume contained in glaciers.

The surface mass balance model is based on a simplified surface energy balance approach, where the contributions by net solar radiation and the combined temperature-dependent fluxes are calculated separately. In addition to examining the effect of anomalies in air temperature and precipitation on the mass balance, we include anomalies in the atmospheric transmissivity. We find that changes in air temperature dominate the glacier volume change, but without the compensating effects of increased precipitation and a lower atmospheric transmissivity, the sea-level contribution would be 35 % higher. The effect of a lower atmospheric transmissivity on the net solar radiation may be compensated by an increase in incoming longwave radiation, which could not be modelled explicitly with our simplified model. For a better understanding of these effects, simulations with more sophisticated surface mass balance models are needed. The finding that projected changes in meteorological variables other than air temperature and precipitation are large enough to affect the surface mass balance and future glacier changes, demonstrates the need to address these processes in more detail.

We find a large spread in the global and regional glacier volume projections for the eight climate models. The spread is primarily related to differences in the projected air temperatures. However, for the Arctic regions in particular, projected changes in precipitation and atmospheric transmissivity also result in considerable variations between the climate model simulations.

This study demonstrates the importance of changes in variables other than air temperature on future glacier volume projections. Future global glacier studies should use more sophisticated surface mass balance models, dynamical glacier models and higher resolution climate input data to improve the estimates of the global glacier contribution to sea-level rise. In addition, detailed mass balance measurements and modelling studies at individual glaciers remain valuable for validation of model results and improvement of model parameterizations.

Acknowledgments We like to thank M. Zemp for providing the glacier mass balance data and the numerous contributors for submitting their measurements to WGMS. The CRU and ECMWF are acknowledged for making their datasets available. We acknowledge the modeling groups, the Program for Climate Model Diagnosis and Intercomparison (PCMDI) and the WCRP's Working Group on Coupled Modelling (WGCM) for their roles in making available the WCRP CMIP3 multi-model dataset. We are grateful to F. Paul, T. Bolch and P. Rastner for their help with the glacier inventory and thank A. Bliss for providing the complete inventory for Antarctica. H. Machguth and M. Schaefer are thanked for providing additional glacier data and A. Slangen is thanked for providing her model results. We like to thank three anonymous reviewers for their constructive comments which helped to improve the manuscript. We acknowledge the ice2sea project, funded by the European Commission's 7th Framework Programme through grant number 226375, ice2sea manuscript number 133.

References

- Arendt A, 77 others (2012) Randolph glacier inventory [v1.0]: a dataset of global glacier outlines. <http://www.glims.org/RGI>. Global Land Ice Measurements from Space, Boulder Colorado, USA
- Bahr DB (1997) Global distributions of glacier properties: a stochastic scaling paradigm. *Water Resour Res* 33:1669–1679
- Bahr DB, Meier MF, Peckham SD (1997) The physical basis of glacier volume-area scaling. *J Geophys Res* 102(B9):20355–20362
- Bliss A, Hock R, Cogley JG (2013) A new inventory of mountain glaciers and ice caps for the Antarctic periphery. *Ann Glaciol* 54:191–199. doi:10.3189/2013AoG63A377
- Chen J, Ohmura A (1990) Estimation of Alpine glacier water resources and their change since the 1870s. *IAHS Publ* 193: 127–135
- Chinn T, Winkler S, Salinger MJ, Haakensen N (2005) Recent glacier advances in Norway and New Zealand: a comparison of their glaciological and meteorological causes. *Geogr Ann* 87A: 141–157
- Cogley JG (2009a) A more complete version of the World Glacier Inventory. *Ann Glaciol* 50:32–38
- Cogley JG (2009b) Geodetic and direct mass-balance measurements: comparison and joint analysis. *Ann Glaciol* 50:96–100
- de Woul M, Hock R (2005) Static mass-balance sensitivity of Arctic glaciers and ice caps using a degree-day approach. *Ann Glaciol* 42:217–224
- Dee DP, 35 others (2011) The ERA-Interim reanalysis: configuration and performance of the data assimilation system. *Q J R Meteorol Soc* 137(656):553–597. doi:10.1002/qj.828
- Dyrgerov MB (2010) Reanalysis of glacier changes: from the IGY to the IPY, 1960–2008. Data of Glaciological Studies, Publication 108, Moscow
- Ettema J, van den Broeke MR, van Meijgaard E, van den Berg WJ, Bamber JL, Box JE, Bales RC (2009) Higher surface mass balance of the Greenland ice sheet revealed by high-resolution climate modeling. *Geophys Res Lett* 36(L12501). doi:10.1029/2009GL038110
- Giesen RH, Oerlemans J (2010) Response of the ice cap Hardangerjøkulen in southern Norway to the 20th and 21st century climates. *Cryosphere* 4:191–213. doi:10.5194/tc-4-191-2010
- Giesen RH, Oerlemans J (2012) Calibration of a surface mass balance model for global-scale applications. *Cryosphere* 6:1463–1481. doi:10.5194/tc-6-1463-2012
- Heikkilä U, Sandvik A, Sorteberg A (2011) Dynamical downscaling of ERA-40 in complex terrain using the WRF regional climate model. *Clim Dyn* 37:1551–1564. doi:10.1007/s00382-010-0928-6
- Huss M, Juvet G, Farinotti D, Bauder A (2010) Future high-mountain hydrology: a new parameterization of glacier retreat. *Hydrol Earth Syst Sci* 14:815–829. doi:10.5194/hess-14-815-2010
- Immerzeel WW, van Beek LPH, Konz M, Shrestha AB, Bierkens MFP (2012) Hydrological response to climate change in a glacierized catchment in the Himalayas. *Clim Change* 110:721–736. doi:10.1007/s10584-011-0143-4
- IPCC (2007) Climate change 2007: the physical science basis. In: Solomon S, Qin D, Manning M, Chen Z, Marquis M, Averyt KB, Tignor M, Miller HL (eds) Contribution of working group I to the 4th assessment report of the intergovernmental panel on climate change. Cambridge University Press, Cambridge
- Jacob T, Wahr J, Pfeffer WT (2012) Recent contributions of glaciers and ice caps to sea level rise. *Nature* 482:514–518. doi:10.1038/nature10847
- Landerer FW, Jungclaus JH, Marotzke J (2007) Regional dynamic and steric sea level change in response to the IPCC-A1B scenario. *J Phys Oceanogr* 37:296–312. doi:10.1175/JPO3013.1
- Marzeion B, Jarosch AH, Hofer M (2012) Past and future sea-level change from the surface mass balance of glaciers. *Cryosphere* 6(6):1295–1322. doi:10.5194/tc-6-1295-2012
- Meehl GA, Covey C, Delworth T, Latif M, McAvaney B, Mitchell JFB, Stouffer RJ, Taylor KE (2007) The WCRP CMIP3 multi-model dataset: a new era in climate change research. *Bull Am Meteorol Soc* 88:1383–1394
- Mihalcea C, Mayer C, Diolaiuti G, D'Agata C, Smiraglia C, Lambrecht A, Vuillermoz E, Tartari G (2008) Spatial distribution of debris thickness and melting from remote-sensing and meteorological data, at debris-covered Baltoro glacier, Karakoram, Pakistan. *Ann Glaciol* 48:49–57
- Mitchell TD, Jones PD (2005) An improved method of constructing a database of monthly climate observations and associated high-resolution grids. *Int J Clim* 25:693–712
- Nakicenovic N, 27 others (2000) IPCC special report on emissions scenarios. Cambridge University Press, Cambridge
- New M, Lister D, Hulme M, Makin I (2002) A high-resolution data set of surface climate over global land areas. *Clim Res* 21:1–25
- Oerlemans J (1991) The mass balance of the Greenland ice sheet: sensitivity to climate change as revealed by energy-balance modelling. *Holocene* 1:40–49
- Oerlemans J, Knap WH (1998) A 1 year record of global radiation and albedo in the ablation zone of Morteratschgletscher, Switzerland. *J Glaciol* 44:231–238
- Oerlemans J, Bassford RP, Chapman W, Dowdeswell JA, Glazovsky AF, Hagen JO, Melvold K, de Ruyter de Wildt M, van de Wal RSW (2005) Estimating the contribution of Arctic glaciers to sea-level change in the next 100 years. *Ann Glaciol* 42:230–236
- Oerlemans J, Giesen RH, van den Broeke MR (2009) Retreating alpine glaciers: increased melt rates due to accumulation of dust (Vadret da Morteratsch, Switzerland). *J Glaciol* 55:729–736
- Pardaens AK, Gregory JM, Lowe JA (2010) A model study of factors influencing projected changes in regional sea level over the twenty-first century. *Clim Dyn* 36:2015–2033. doi:10.1007/s00382-009-0738-x
- Paul F, Kääb A, Maisch M, Kellenberger T, Haeblerli W (2004) Rapid disintegration of Alpine glaciers observed with satellite data. *Geophys Res Lett* 31(L21402). doi:10.1029/2004GL020816
- Pelto MS (2006) The current disequilibrium of North Cascade glaciers. *Hydrol Proc* 20(4):769–779. doi:10.1002/hyp.6132
- Radić V, Hock R (2010) Regional and global volumes of glaciers derived from statistical upscaling of glacier inventory data. *J Geophys Res* 115(F01010). doi:10.1029/2009JF001373
- Radić V, Hock R (2011) Regionally differentiated contribution of mountain glaciers and ice caps to future sea-level rise. *Nat Geosci* 4:91–94. doi:10.1038/NNGEO1052
- Raper SCB, Braithwaite RJ (2006) Low sea level rise projections from mountain glaciers and icecaps under global warming. *Nature* 439:311–313. doi:10.1038/nature04448
- Rasmussen LA, Conway H (2005) Influence of upper-air conditions on glaciers in Scandinavia. *Ann Glaciol* 42:402–408
- Scherler D, Bookhagen B, Strecker MR (2011) Spatially variable response of Himalayan glaciers to climate change affected by debris cover. *Nat Geosci* 4:156–159. doi:10.1038/ngeo1068
- Slangen ABA, van de Wal RSW (2011) An assessment of uncertainties in using volume-area modelling for computing the twenty-first century glacier contribution to sea-level change. *Cryosphere* 5:673–686. doi:10.5194/tc-5-673-2011
- Slangen ABA, Katsman CA, van de Wal RSW, Vermeersen LLA, Riva REM (2012) Towards regional projections of twenty-first century sea-level change based on IPCC SRES scenarios. *Clim Dyn* 38:1191–1209. doi:10.1007/s00382-011-1057-6
- Stahl K, Moore RD, Shea JM, Hutchinson D, Cannon AJ (2008) Coupled modelling of glacier and streamflow response to future

- climate scenarios. *Water Resour Res* 44(W02422). doi:[10.1029/2007WR005956](https://doi.org/10.1029/2007WR005956)
- Urrutia R, Vuille M (2009) Climate change projections for the tropical Andes using a regional climate model: temperature and precipitation simulations for the end of the 21st century. *J Geophys Res* 114(D02108). doi:[10.1029/2008JD011021](https://doi.org/10.1029/2008JD011021)
- World Glacier Monitoring Service (WGMS) (1999, updated 2012) World Glacier Inventory, Antarctica. doi:[10.7265/N5/NSIDC-WGI-2012-02](https://doi.org/10.7265/N5/NSIDC-WGI-2012-02), National Snow and Ice Data Center, Boulder Colorado, USA
- Zemp M, Nussbaumer SU, Gärtner-Roer I, Hoelzle M, Paul F, Haeberli W (eds) (2011) Glacier mass balance bulletin no. 11 (2008–2009). ICSU(WDS)/IUGG(IACS)/UNEP/UNESCO/WMO, World Glacier Monitoring Service, Zurich, Switzerland